# Curb Detection Method Based on Curvatures for Urban Autonomous Navigation

C. Fernández, D. F. Llorca, C. Stiller, M. A. Sotelo

*Abstract*— This paper addresses the problem of curb detection for ADAS or autonomous navigation in urban scenarios. The algorithm is based on clouds of 3D points and it is evaluated using 3D information from a pair of stereo cameras and also from a LIDAR. The feature to detect the curbs is the curvature of the road surface. The curvature estimation requires a dense point cloud, therefore the density of the LIDAR cloud has been increased using Iterative Closest Point (ICP) with the previous scans. The proposed algorithm can deal with curbs of different curvature and heights, from as low as 3 cms, in a range up to 20 m if the curbs are connected in the curvature image. The parameters of the curb are modeled with lines and lateral error is compared to a ground truth. The ground truth sequences were manually labeled by an expert and they are publicly available for the community.

## I. INTRODUCTION AND RELATED WORK

Road detection has been of the most important topics in fields of Advanced Driver Assistance Systems (ADAS) and autonomous driving. In the last years ADAS have been improving to achieve autonomous driving. Nowadays, some production vehicles are equiped with systems that take the control of the vehicle to reduce the damage to the occupants in case of accident. All these systems require an accurate scene understanding. For such purpose, vision sensors have been used by the automotive industry in diverse systems. For example, lane departure warning and lane keeping systems. This kind of systems are consolidated in today's cars. However their use is limited to highways and roads with clearly visible lane markers. The improvement of these systems for unmarked roads and urban environments is still a challenge. In most of the non urban roads, the free space is limited by road markings. However, metropolitan areas are more complex, and the free space can be restricted by road markings, parked cars, traffic signs, lampposts and curbs of quite different heights. The accuracy and reliability of vision based systems are strongly affected by the large variety of street configurations, different materials and textures, illumination changes, etc.

In order to solve this adversities, research resources must be oriented to developing algorithms for a reliable detection of the curbs and road edges, see Figure 1. This paper is focused on curb detection for urban scenarios. We propose a method based on the curvature estimation and it is evaluated with 3D point clouds captured from stereo vision and

C. Fernández, D. F. Llorca and M. A. Sotelo are with the Computer Engineering Department, Polytechnic School, University of Alcalá, Madrid, Spain. email: carlos.fernandez, llorca, sotelo@aut.uah.es. Christoph Stiller is Professor and Director of the Institute of Measurement and Control Systems at Karlsruhe Institute of Technology, Karlsruhe, Germany. email: stiller@kit.edu

LIDAR. The free space is a very important knowledge to understand the current scenario and it provides information to the pathplanning module and other components of an autonomous vehicle. A curb detection system can be applied to a pedestrian crossing prediction system. In [1], one of the features in their proposed prediction model is the distance between the pedestrian and the curb.
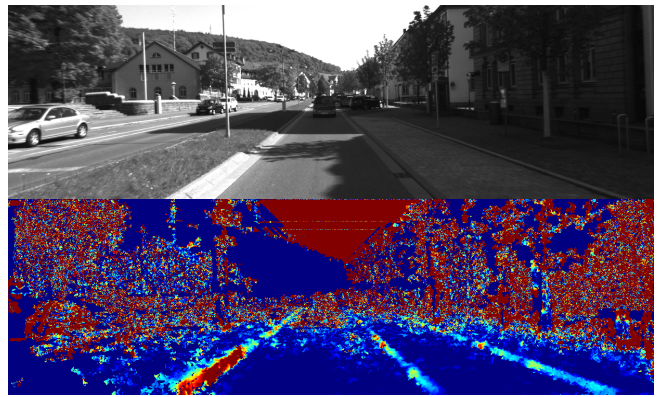


Fig. 1. Example of a complex urban scenario. On the left side, the scene has a big curb in the closer distance and a lower one further. On the right side, there are two small curbs, the first limits the parking place and the second one limits the sidewalk.

In situations where no lane markings or curbs are present in the scene, texture and color information are inherent features to designate the road. The Hue Saturation Intensity (HSI) color space is used in [2] and [3] together with road shape restrictions. An important issue for vision based systems, is the presence of shadows in the scene. In [4] an illuminant invariant image is obtained to remove the influence of the light changes. This illuminant invariant image is applied in road detection in [5] and [6]. Firstly, patches are extracted from monocular images and they are analyzed to find local visual properties for a metric confidence map. Secondly, features called SPatial RAY (SPRAY) are computed on the confidence map. Afterwards, the ego-lane is extracted applying a semantic segmentation.

In other cases LIDAR enhances vision systems. In [7], the authors propose a free space and speed humps detection system based on LIDAR and a monocular camera. Generally monocular based systems are less robust than stereo-vision for road structure reconstruction. Consequently, in [8] a semantic graph associated with a stereo-based homography is proposed, where the road edges are located using the Viterbi algorithm. As a continuation of the previous work [9], the authors propose to solve the homography as a maximum

a posteriori (MAP) problem in a Markov Random Field (MRF) that computes the binary labels road/non-road and it learns the optimal parameters for the probabilistic algorithm. The stereo vision matching algorithm is an important stage of a stereo system. The disparity mismatching produces unexpected results, therefore in [10] the authors propose a model of arbitrarily orient slanted planes to improve road surface estimation.

In [11], Loopy Belief Propagation are used to assign points extracted from the 3D point cloud to curb adjacent surfaces. As a consequence, the reconstruction of the curbs can be done even in low height curbs up to 20 meters. An improvement of the previous work is presented in [12], where the authors include a temporal filter to improve the accuracy and robustness. More recently, an impressive system has been deployed in [13] based on the sole use of vision, radar, and accurate digital maps for autonomous driving on all types of scenarios, including rural roads, small villages and major cities. For such purpose, visual clues were off-line obtained and learned in order to develop a really robust self-localization system capable of inferring the road structure in an accurate way. The system successfully traversed more than 100 km in a driverless mode along german roads and cities.

In this paper we propose an algorithm for road curb detection based on curvature surface estimation in 3D point clouds. The clouds can be captured from different types of sensors, for example LIDAR or stereo cameras. The point cloud from LIDAR is sparse because of the vertical resolution. In order to increase the cloud density, an iterative algorithm is applied to align the last scans. The proposed method is included in a more complex system of urban autonomous driving with particular emphasis on unmarked roads. The rest of the paper is structured as follows: section II presents a general description of the system, including the methods for the curvature estimation, curb detection and point cloud upsampling. Results and discussion are presented in section III. Finally, we analyze our conclusions and future work in section IV.

## II. SYSTEM DESCRIPTION

### A. General Description

In this paper, a curb detection method based on surface curvature is compared using two different inputs: The first one is a 3D reconstruction using the Semi Global Matching (SGM) stereo matching algorithm [14] and the second one is the 3D reconstruction from LIDAR.

This paper is focus on urban environments, therefore, the performance of the system is evaluated using the public dataset: KITTI Vision Benchmark Suite. [15], [16]. The dataset provides information of urban scenarios from different types of sensors, such as monochrome and color cameras, multilayer LIDAR, GPS and IMU. Some details of those sensors are: 2 Grayscale cameras 1.4 Mpx (Point Grey Flea 2), 2 Color cameras 1.4 Mpx (Point Grey Flea 2), 4 Varifocal lenses, 4-8 mm (Edmund Optics NT59-917), Laserscanner

(Velodyne HDL 64E) and Inertial Navigation System (OXTS RT 3003).

The height of the cameras is 1.65 meters and the height of the LIDAR is 1.73 meters. Furthermore, the LIDAR is installed 27 centimeters behind the cameras, consequently the relationship between camera and LIDAR poses should be calibrated. The baseline for the stereo vision is 0.54 meters hence the 3D reconstruction can deal with long distances.

On the one hand, road scene reconstruction from stereo is more dense than LIDAR reconstruction but it is also affected by mismatching errors. On the other hand, LIDAR provides low noise measurements at long range distance but depending on the vertical resolution, the reconstruction is sparse.

### B. Curvature Estimation

The proposed curb detection method is based on surface curvature estimation presented in [17] and [18]. This feature has been also used in [19] for free space detection. The curvature describes the variation along the surface normal and it varies between 0 and 1, where low values correspond to flat surfaces. The curvature feature is more robust and stable than tangent plane normal vectors. For each point $p$, the nearest neighbors (NN) $p_i$ in a surrounding area defined by a radius $R$ are selected. These points are used to create a weighted covariance matrix, where $k$ denotes the number of NN.

$$\bar{p} = \frac{1}{k}\sum_{i=1}^{k} p_i \; ; \; \mu = \frac{1}{k}\sum_{i=1}^{k} |\bar{p} - p_i| \qquad (1)$$

$$w_i = exp\left(-\frac{(p - p_i)^2}{\mu^2}\right) \qquad (2)$$

$$C = \sum_{i=1}^{k} w_i \cdot (p_i - \bar{p})^T \cdot (p_i - \bar{p}) \qquad (3)$$

The weight for the inliers is $w_i = 1$ and the weight for the outliers is calculated using equation 2 where $\mu$ is the mean distance from the current point $p$ to all its neighbors $p_i$. The eigenvector $V$ and eigenvalues $\lambda$ are computed as $C \cdot V = \lambda \cdot V$. The curvature $\gamma_z^p$ is defined by equation 4, where $\lambda_x \leq \lambda_y \leq \lambda_z$ are the eigenvalues of the covariance matrix $C$.

$$\gamma_z^p = \frac{\lambda_z}{\lambda_x + \lambda_y + \lambda_z} \qquad (4)$$

### C. Curb Detection

In our reference system, the $Z$ axis is orthogonal to the road, therefore the curvature $\gamma_z$ provides very discriminant description of the road shape. Curb height and curvature $\gamma_z$ are highly correlated, consequently after a thorough observation of urban scenes in the KITTI dataset, a set of thresholds $\alpha_i = \{1 \ldots N\}$ is used to label the type of curb, see Table I:

Curb curvature is different in each scene. For example, if the curb is a regular one, most of the points exhibit curvature values $\gamma_z \in [\alpha_2, \alpha_3)$, but there are also some curb points yielding significantly different values, see Figure 2(b). These
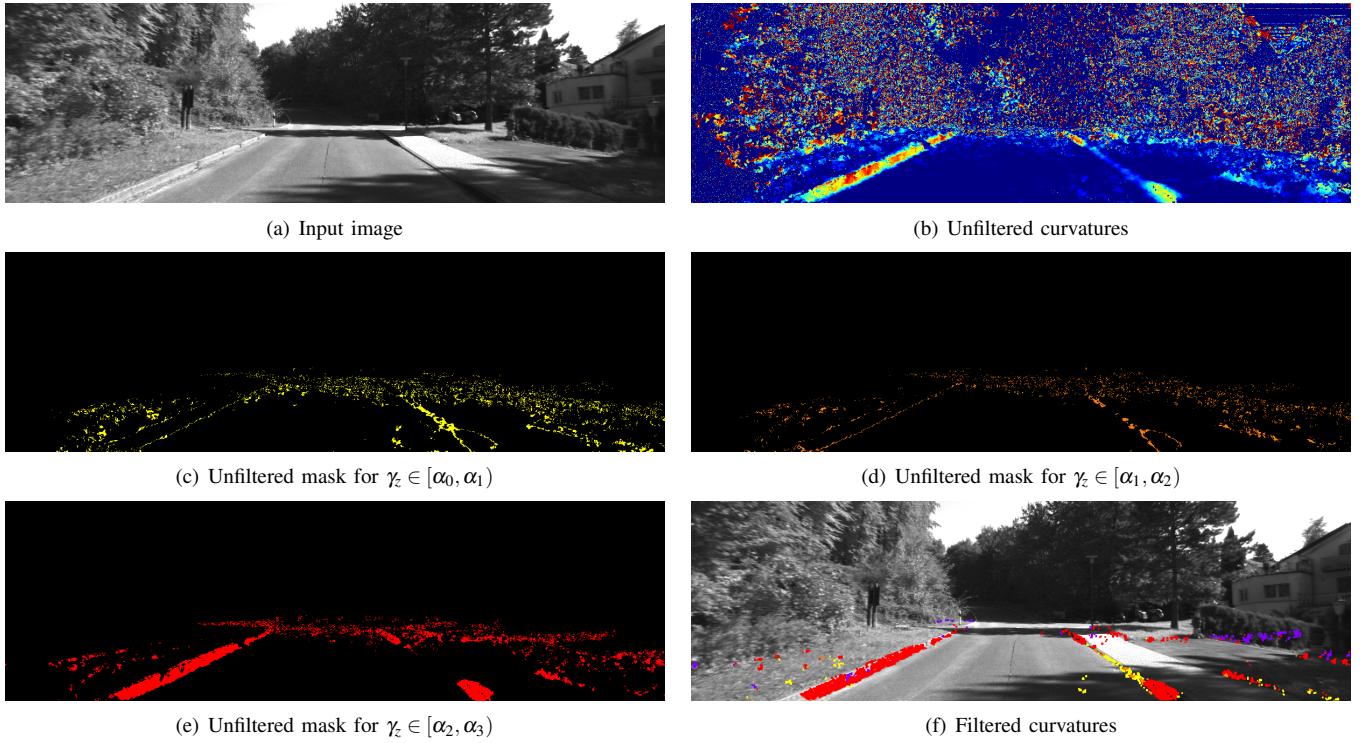
(a) Input image



(b) Unfiltered curvatures



(c) Unfiltered mask for $\gamma_z \in [\alpha_0, \alpha_1)$



(d) Unfiltered mask for $\gamma_z \in [\alpha_1, \alpha_2)$



(e) Unfiltered mask for $\gamma_z \in [\alpha_2, \alpha_3)$



(f) Filtered curvatures

Fig. 2.   Filtering process of the input noisy curvatures and the final result.

TABLE I

CURB CURVATURE VALUES

| DESCRIPTION | CURVATURE | COLOR |
|---|---|---|
| Flat surface | $0 \leq \gamma_z < \alpha_0$ | not painted |
| Very Small Curbs ($\sim$3 cm) | $\alpha_0 \leq \gamma_z < \alpha_1$ | yellow |
| Small Curbs ($\sim$5 cm) | $\alpha_1 \leq \gamma_z < \alpha_2$ | orange |
| Regular Curbs ($\sim$10 cm) | $\alpha_2 \leq \gamma_z < \alpha_3$ | red |
| Big Obstacles | $\alpha_3 \leq \gamma_z \leq 1$ | purple |

measurement outliers are removed by means of a filtering process. A binary mask is processed for each curvature range using morphological operations and contour analysis. The resulting masks are merged and refiltered in order to get an image like the one shown in Figure 2(f). The use of fixed or empirical thresholds is then avoided given that the proposed function is adapted automatically for different scenes depending on the dominant curvature value.

### D. Increase Cloud Density

The point cloud from the stereo is dense, however the LIDAR cloud is sparse because the vertical resolution is 0.4 degrees and the algorithm described in Section II-C can not be applied. The cloud requires to be dense, for this reason, for every point, the nearest neighbors (NN) are fitted to a surface and new points are generated on it. If the road surface is estimated using a polynomial, in presence of small curbs it smooths the real shape of the scene and the small curbs are partially removed. To avoid this problem an iterative algorithm is applied to align the sparse clouds from instant $t-n$ to $t$ and create a dense cloud. This algorithm is Iterative

Closest Point (ICP) [20], [21].

**Data**: point cloud $A = \{a_1, \ldots, a_M\}$, point cloud
$\qquad B = \{b_1, \ldots, b_N\}$, initialized matrix T.
**Result**: The transformation matrix T which aligns A
$\qquad$ and B.
**while** *not converged* **do**
$\qquad$ **for** $i = 1$ **to** $N$ **do**
$\qquad\qquad m_i = FindClosestPointInA(Tb_i)$
$\qquad\qquad$ **if** $\|m_i - Tb_i\| \leq d_{max}$ **then**
$\qquad\qquad\qquad w_i = 1$
$\qquad\qquad$ **else**
$\qquad\qquad\qquad w_i = 0$
$\qquad\qquad$ **end if**
$\qquad$ **end for**
$\qquad T = argmin(\sum w_i \|Tb_i - m_i\|^2)$
**end**

**Algorithm 1:** Standard ICP

The algorithm is illustrated in Algorithm 1. ICP minimizes the difference between two point clouds iteratively. The first one $A$ is kept fixed and the other one $B$ is transformed to match the reference. If the clouds are close to each other, the initial values for $T$ can be set to identity. For each iteration, every point in $B$ is transformed with the current transformation matrix $T$ and matched with the corresponding point in $A$. If the distance between the points is greater than $d_{max}$, the points are rejected. As depicted in Figure 3, the ICP algorithm does not smooth the original data and the small curbs can still be detected with the algorithm explained in
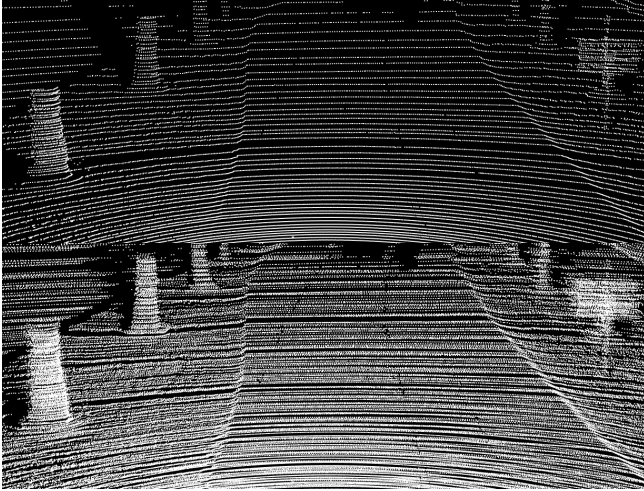
Section II-C.



Fig. 3. Result of the Iterative Closest Point algorithm for the last 5 spins of the LIDAR.
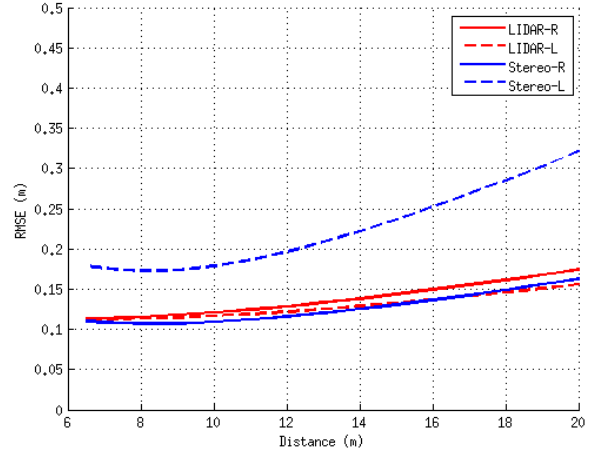


Fig. 4. Lateral RMSE obtained comparing ground truth and the result of the algorithm. The results for left and right curbs are separated to evaluate the performance individually.

## III. RESULTS

The lateral accuracy was evaulated in sequences of the KITTI dataset. In that dataset there is not any specific ground truth for curbs detection. A contribution of this paper is a public dataset containing some sequences with manually labeled curbs. The ground truth was annotated by an expert in the image and also in the LIDAR data. The number of sequences labeled will be increased soon. The dataset is publicly available at www.isislab.es and if you use the dataset in your research, please cite this paper.

For the evaluation, straight lines are fitted to the detected curb points and also to the labeled ground truth points. The estimated line and the ground truth are defined by the points $p$ and $q$ and the direction vectors $\vec{u}$ and $\vec{v}$ respectively. The accuracy is evaluated by computing equation 7, where $a$ and $b$ are the evaluated range, from 6 up to 20 meters. In urban scenarios the driving speed is low and we consider that 20 meters is enough to manoeuvre safely.

$$l = \frac{u_y}{u_x}(x - p_x) + p_y \tag{5}$$

$$\widehat{l} = \frac{v_y}{v_x}(x - q_x) + q_y \tag{6}$$

$$RMSE = \sqrt{\frac{1}{b-a}\int_a^b (l - \widehat{l})^2 dx} \tag{7}$$

In the case of the stereo data, the disparity images are computed using Semi Global Matching (SGM). This method is based on the idea of pixelwise matching of mutual information and approximation of a global 2D smoothness constraint by combining many 1D constraints. Accumulating the last 5 spins of the LIDAR, the cloud density is good enough to estimate the curvatures. The density of the LIDAR cloud is increased using ICP, therefore some errors during the matching stage can yield point clouds with slightly worse

quality than a dense stereo point cloud. In Figure 4, the lateral error is depicted. The LIDAR error is plotted in red and the error from the stereo is plotted in blue. The performance of the algorithm using the LIDAR data as input is very similar comparing the curb on the left and the curb on the right. In addition, the performance using the 3D data from the stereo is also similar to LIDAR. However, the lateral error on the left curb is significantly higher.

Analysing the disparity images of several sequences we realised that the cameras are not well calibrated. For this reason, the left part of the image provides noisy and unrealistic 3D information, see Figure 5. As shown in Figure 4, when the stereo is well calibrated, the performance of the stereo is even better than the LIDAR because is more dense than the LIDAR, therefore we demonstrate that the use of stereo cameras for ADAS in urban environments is a good technology. The curb detection algorithm presents a lateral RMSE of 12cm in a range of 6 to 20 meters distance but the error on the left side is 22cm.

## IV. CONCLUSIONS AND FUTURE WORKS

In this paper a curb detection estimation algorithm based on 3D point clouds has been presented. The use of fixed or empirical thresholds is avoided given that the proposed function is adapted automatically for different scenes depending on the dominant curvature value.

A public dataset of manually labeled curbs is available at www.isislab.es. If you use the dataset in your research, please cite this paper. The algorithm presented in this paper is valid for straight and curved curbs, however a geometric detection method is not enough to get a robust free space detection system due to the fact that some road limits have the same height as the road. For this reason texture and color provide very important information that complements to the geometric reconstruction. For future work, a new machine learning approach will include the geometric reconstruction
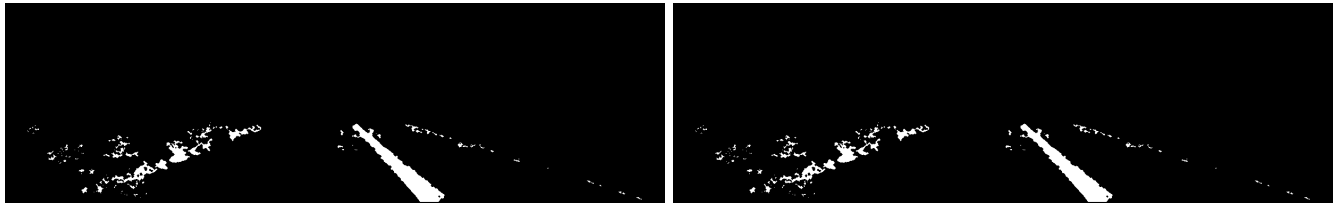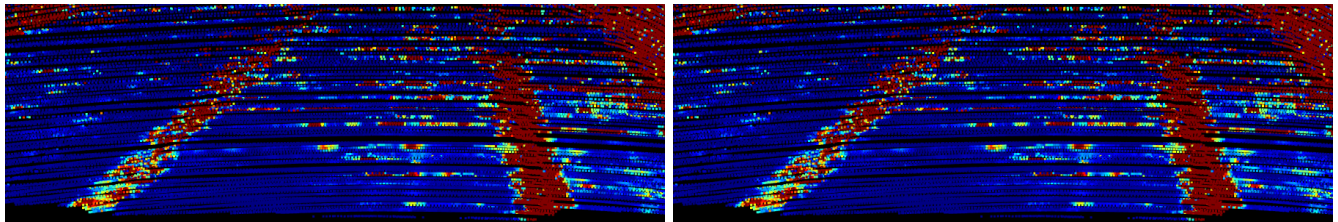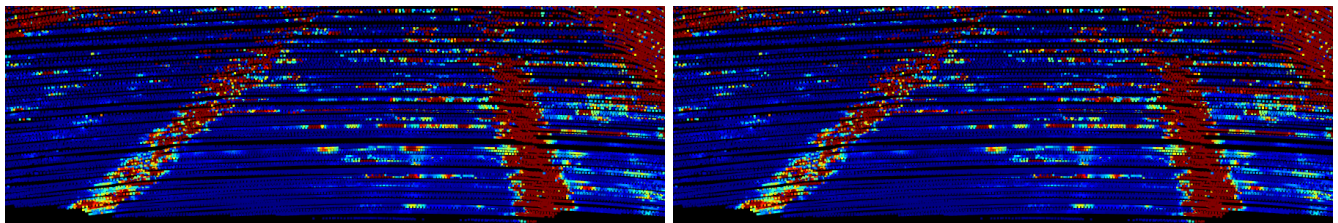
(a) Greyscale image
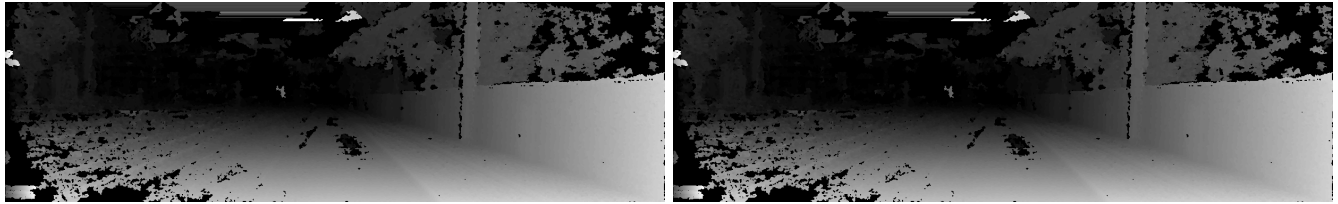

(b) Disparity image
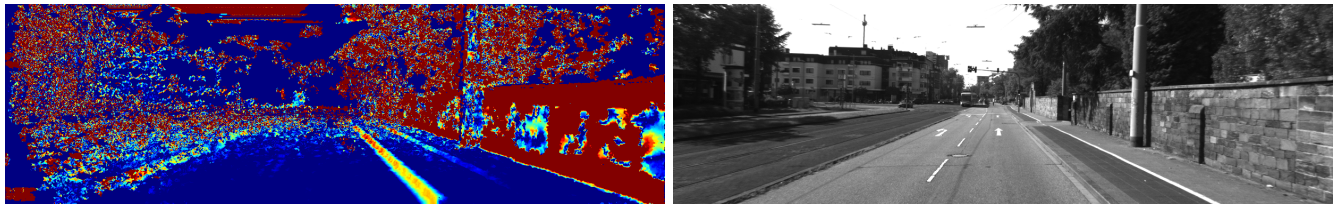

(c) Curvature estimation using stereo point cloud


(d) Output of the curb detection algorithm for the stereo point cloud


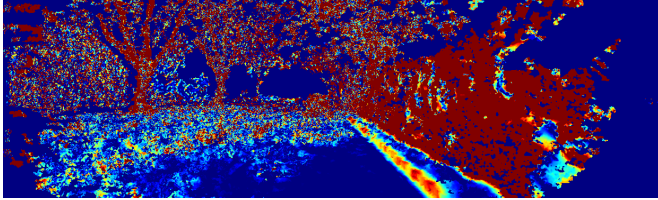(e) Curvature estimation using LIDAR point cloud


(f) Output of the curb detection algorithm for the LIDAR point cloud
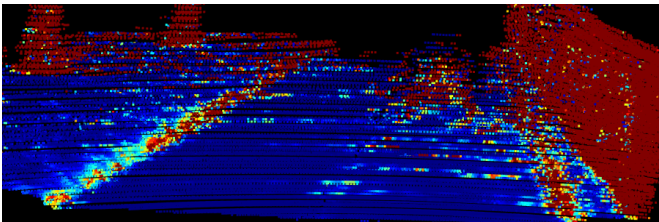
Fig. 6.    Comparison of curvature estimation. The stereo results have more noise than LIDAR.

(a) Greyscale image of the analyzed frame



(b) Curvature estimation using 3D stereo data



(c) Curvature estimation using LIDAR data

Fig. 5. Comparison of curvature estimation. Stereo calibration and mismatching errors produces wrong surface reconstruction on the left side of the image.

presented in this paper and also texture and color information to detect the drivable area.

The proposed algorithm is compared using different origins of the 3D cloud data. The LIDAR cloud is more robust to noise than the stereo cloud, however the LIDAR cloud is sparse. In order to improve the LIDAR cloud density, the Iterative Closest Point (ICP) is applied. The resulted cloud has the advantage of the stereo density and also the robustness of the LIDAR. Another advantage of that cloud is the reflectivity measurements. The LIDAR cloud provides apart of 3D measurements, reflectivity measurements. The reflectivity is very usefull to detect traffic signs and road marking during daytime and nighttime. For future work, an algorithm for road marking detection will be developed using LIDAR jointly with cameras.

## V. ACKNOWLEDGMENTS

## REFERENCES

[1] S. Bonnin, T. Weisswange, F. Kummert, and J. Schmuedderich, "Pedestrian crossing prediction using multiple context-based models," in *Intelligent Transportation Systems (ITSC), 2014 IEEE 17th International Conference on*, Oct 2014, pp. 378–385.

[2] M. A. Sotelo, F. J. Rodriguez, and L. Magdalena, "Virtuous: vision-based road transportation for unmanned operation on urban-like scenarios," *IEEE Transactions on Intelligent Transportation Systems*, vol. 5, no. 2, pp. 69–83, June 2004.

[3] M. A. Sotelo, F. J. Rodriguez, L. Magdalena, L. M. Bergasa, and L. Boquete, "A color vision-based lane tracking system for autonomous driving on unmarked roads," *Autonomous Robots*, vol. 16, no. 1, pp. 95–116, 2004.

[4] G. Finlayson, S. Hordley, C. Lu, and M. Drew, "On the removal of shadows from images," *IEEE Transactions on Pattern Analysis and Machine Intelligence*, vol. 28, no. 1, pp. 59–68, Jan 2006.

[5] J. Alvarez and A. Lopez, "Road detection based on illuminant invariance," *IEEE Transactions on Intelligent Transportation Systems*, vol. 12, no. 1, pp. 184–193, March 2011.

[6] J. Fritsch, T. Kuhnl, and F. Kummert, "Monocular road terrain detection by combining visual and spatial information," *IEEE Transactions on Intelligent Transportation Systems*, vol. PP, no. 99, pp. 1–11, 2014.

[7] C. Fernandez, M. Gavilan, D. Llorca, I. Parra, R. Quintero, A. Lorente, L. Vlacic, and M. Sotelo, "Free space and speed humps detection using lidar and vision for urban autonomous navigation," in *Intelligent Vehicles Symposium (IV), 2012 IEEE*, June 2012, pp. 698–703.

[8] C. Guo, T. Yamabe, and S. Mita, "Robust road boundary estimation for intelligent vehicles in challenging scenarios based on a semantic graph," in *IEEE Intelligent Vehicles Symposium (IV)*, June 2012, pp. 37–44.

[9] C. Guo, S. Mita, and D. McAllester, "Robust road detection and tracking in challenging scenarios based on markov random fields with unsupervised learning," *IEEE Transactions on Intelligent Transportation Systems*, vol. 13, no. 3, pp. 1338–1354, Sept 2012.

[10] B. Ranft and T. Strauss, "Modeling arbitrarily oriented slanted planes for efficient stereo vision based on block matching," in *Intelligent Transportation Systems (ITSC), 2014 IEEE 17th International Conference on*, Oct 2014, pp. 1941–1947.

[11] J. Siegemund, D. Pfeiffer, U. Franke, and W. Frstner, "Curb reconstruction using conditional random fields," in *IEEE Intelligent Vehicles Symposium (IV)*, June 2010, pp. 203–210.

[12] J. Siegemund, U. Franke, and W. Frstner, "A temporal filter approach for detection and reconstruction of curbs and road surfaces based on conditional random fields," in *IEEE Intelligent Vehicles Symposium (IV)*, June 2011, pp. 637–642.

[13] J. Ziegler, P. Bender, M. Schreiber, H. Lategahn, T. Strauss, C. Stiller, T. Dang, U. Franke, N. Appenrodt, C. Keller, E. Kaus, R. Herrtwich, C. Rabe, D. Pfeiffer, F. Lindner, F. Stein, F. Erbs, M. Enzweiler, C. Knoppel, J. Hipp, M. Haueis, M. Trepte, C. Brenk, A. Tamke, M. Ghanaat, M. Braun, A. Joos, H. Fritz, H. Mock, M. Hein, and E. Zeeb, "Making bertha drive?an autonomous journey on a historic route," *IEEE Intelligent Transportation Systems Magazine*, vol. 6, no. 2, pp. 8–20, Summer 2014.

[14] H. Hirschmuller, "Accurate and efficient stereo processing by semi-global matching and mutual information," in *Proceedings of the 2005 IEEE Computer Society Conference on Computer Vision and Pattern Recognition (CVPR'05)*. Washington, DC, USA: IEEE Computer Society, 2005, pp. 807–814.

[15] A. Geiger, P. Lenz, and R. Urtasun, "Are we ready for autonomous driving? the kitti vision benchmark suite," in *Conference on Computer Vision and Pattern Recognition (CVPR)*, 2012.

[16] A. Geiger, P. Lenz, C. Stiller, and R. Urtasun, "Vision meets robotics: The kitti dataset," *International Journal of Robotics Research (IJRR)*, 2013.

[17] R. B. Rusu, Z. C. Marton, N. Blodow, M. Dolha, and M. Beetz, "Towards 3d point cloud based object maps for household environments," *Robot. Auton. Syst.*, vol. 56, no. 11, pp. 927–941, Nov. 2008.

[18] M. Pauly, M. Gross, and L. Kobbelt, "Efficient simplification of point-sampled surfaces," in *Visualization, 2002. VIS 2002. IEEE*, Nov 2002, pp. 163–170.

[19] C. Fernandez, R. Izquierdo, D. Llorca, and M. Sotelo, "Road curb and lanes detection for autonomous driving on urban scenarios," in *Intelligent Transportation Systems (ITSC), 2014 IEEE 17th International Conference on*, Oct 2014, pp. 1964–1969.

[20] S. Rusinkiewicz and M. Levoy, "Efficient variants of the icp algorithm," in *3-D Digital Imaging and Modeling, 2001. Proceedings. Third International Conference on*, 2001, pp. 145–152.

[21] M. Greenspan and M. Yurick, "Approximate k-d tree search for efficient icp," in *3-D Digital Imaging and Modeling, 2003. 3DIM 2003. Proceedings. Fourth International Conference on*, Oct 2003, pp. 442–448.